

Single-crystals of magnesium sulfite hexahydrate doped with nickel – structure, density and optical properties

G. Giorgi¹, G. L. Lyutov², L. G. Lyutov^{2*}

¹ *Universita Degli Studi di Siena – via A. Moro – 53100 Siena, Italy; e-mail: ciads@unisi.it*

² *Sofia University “St. Kl. Ohridski”, J. Bourcher st. 1, Sofia, Bulgaria*

Received January 28, 2011; Revised April 22, 2011

MgSO₃·6H₂O is a crystalline compound which possesses notable optical properties, which make possible its application in modern high technologies. Single-crystals of the compound can be obtained by method which combines chemical reaction and polythermic growth from low-temperature water-based solutions.

The crystallization process can be best started at temperatures 53–46 °C. At higher temperatures MgSO₃·6H₂O is prone to turn into MgSO₃·3H₂O. Crystal growth lasts 20–25 days, where the temperature is gradually lowered to ambient by semi-automatic device.

The apparatus allows growth of crystals with maximum length of the basal edge of trigonal pyramid 30–40 mm.

For a first time we have started research on single-crystal growth of MgSO₃·6H₂O with isomorphic inclusion of Ni²⁺ and Co²⁺ ions. It is supposed that these ions would influence the main physical and optical properties of the crystals, such as refractive index, range of optical transparency, magneto-optical properties etc. We have obtained single crystals of MgSO₃·6H₂O with included 2–5% Ni²⁺ ions, where nickel is added by NiCl₂·6H₂O. The process starts with mixing the Mg- and Ni- bearing solution with the one containing SO₃²⁻ and S₂O₅²⁻ at 50–60 °C, followed by gradual cooling the joint-solution until it reaches room temperature for a few days.

Key words: MgSO₃·6H₂O, doping, Ni²⁺, PACS: birefringence – solids – 78.20.F, density – crystalline solids – 71.20, diffraction – X-ray analysis – 61.10.H, structure – crystalline solids – 61.66.

1. INTRODUCTION

Co-crystallization depends on chemical correlation matrix – admixtures. Typical cases are shown in [1].

Co-crystallization of isomorphic and isodimorphic admixtures

Isomorphic compounds are compounds which have similar composition and crystallize in the same or similar form. In isomorphic compounds, mutual replacement of equivalent particles happens, in equivalent positions within the crystal structure. Solid solutions form by replacement in such way. In isodimorphic compounds, phase transition happens in which the admixture takes the structure of the main component. For example the compounds NiSO₄·7H₂O (rhombohedral), CoSO₄·7H₂O (monoclinic) and CuSO₄·5H₂O (triclinic) can form mixed crystals, where the admixture accepts the unstable (for it) structure of the macro-component.

Co-crystallization of non-isomorphic admixtures

Non-isomorphic are ions which have different charges or different chemical characteristics. They are not replacements within the crystal structure but they are adsorbed on the surfaces of the growing crystals. That adsorption is selective and inclusion is on sectors. Such inclusions alter the shape of the crystal, because the inclusions change the speed of growth of the crystal in some directions.

Complex compounds can form well-shaped crystals, which include micro-admixtures (anomalous mixed crystals). Ions with higher charge can displace ions with lower charge near cation vacancy, thereby preserving general electro-neutrality. Such inclusion is called “hetero-valent isomorphism”. That phenomenon can be used to dope crystals with admixtures, thereby giving them desired properties for usage in scintillators, lasers, piezoelectric and segnetoelectric elements.

Isotherms of co-crystallization of various systems are shown on Figure 1, where:

* To whom all correspondence should be sent:
E-mail: nhll@chem.uni-sofia.bg

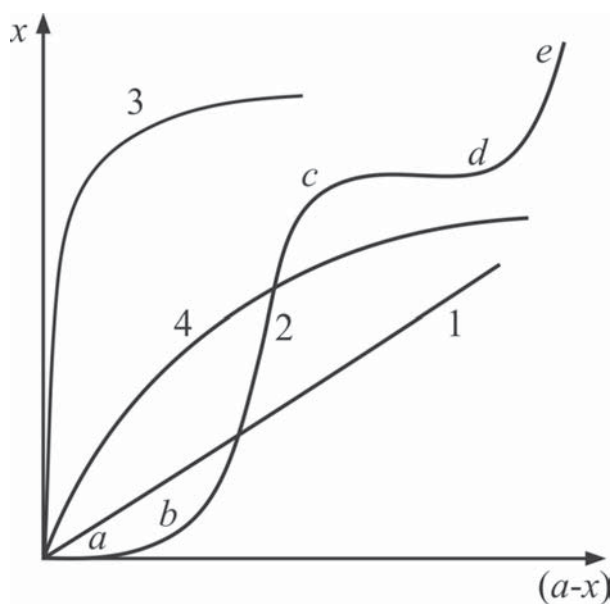


Fig. 1. Isotherms of co-crystallization of various systems. 1 – isomorphic and isodimorphic; 2 – anomalous mixed crystals with lower limit of inclusion; 3 – complex compounds of non-isomorphic admixtures; 4 – adsorption inclusion

Line 1 – Isotherm of co-crystallization of ideal mixed crystals. Equilibrium coefficient of co-crystallization can be gauged from the slope of line 1.

Line 2 – Isotherm of co-crystallization of anomalous mixed crystals, which shows the lower boundary of inclusion (*a-b*), rapid growth of the included amount (*b-c*), saturation, where the included amount does not change (*c-d*) and then sharp rapid growth of the included admixture amount (*d-e*).

Line 3 – Isotherm of co-crystallization of anomalous mixed crystals where complex ligands with high electric charge form new nucleus.

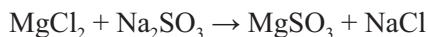
Line 4 – adsorption-based inclusion without lower boundary, observed in some rarely encountered systems.

2. EXPERIMENTAL

2.1. Method

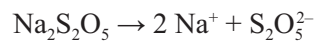
Single-crystals of the compound can be obtained by method which combines chemical reaction and polythermic growth from low-temperature water-based solutions.

The chemical reaction is as follows [2]:



where, in order to prevent mass crystallization, HSO_3^- ions are added. They apparently widen the metastable zone and hinder the process by increasing

solubility. HSO_3^- ions can be brought into the system by adding $\text{Na}_2\text{S}_2\text{O}_5$ as follows:



The crystallization process is the best to start at temperature 46–53 °C. At higher temperatures $\text{MgSO}_3 \cdot 6\text{H}_2\text{O}$ is prone to turn into $\text{MgSO}_3 \cdot 3\text{H}_2\text{O}$. Crystal growth lasts 20–25 days, where the temperature is gradually lowered to ambient by a semi-automatic device.

The apparatus allows growth of crystals with maximum length of the basal edge of trigonal pyramid 30–40 mm.

We have obtained single crystals of $\text{MgSO}_3 \cdot 6\text{H}_2\text{O}$ with included 2–5% Ni^{2+} ions, where nickel is added by $\text{NiCl} \cdot 6\text{H}_2\text{O}$. The process starts with mixing the Mg- and Ni-bearing solution with the one containing SO_3^{2-} and $\text{S}_2\text{O}_5^{2-}$ at 50–55 °C, followed by gradual cooling the joint-solution until it reaches room temperature for a few days.

Polythermic single-crystal growth from low-temperature water-based solutions. In polythermic methods supersaturation is achieved by relying on Van-t-Hoff's equation, which is valid in most cases:

$$\frac{d \ln C}{dT} = \frac{\Delta H}{RT^2}$$

where: C – solubility (in mol parts), T – absolute temperature [°K], ΔH – enthalpy of dissolving, R – gas constant

When $\Delta H > 0$, $\frac{d \ln C}{dT} > 0$, the solubility (C) rises with temperature (T) and vice versa, as it is shown in Figure 2 (with continuous line).

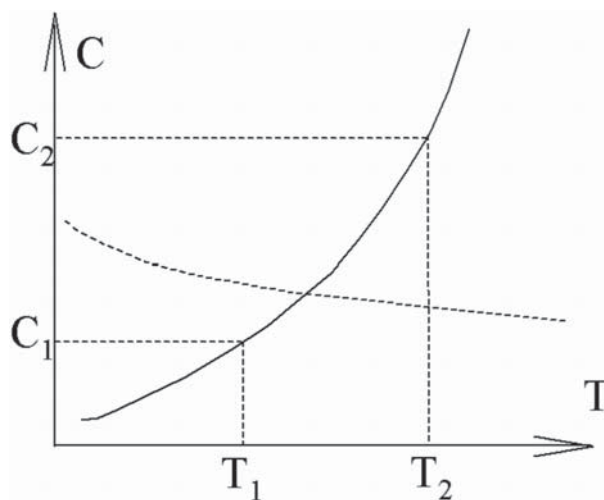


Fig. 2. Trend of solubility in dependence of temperature – $\Delta H > 0$ (continuous line) and $\Delta H < 0$ (broken line)

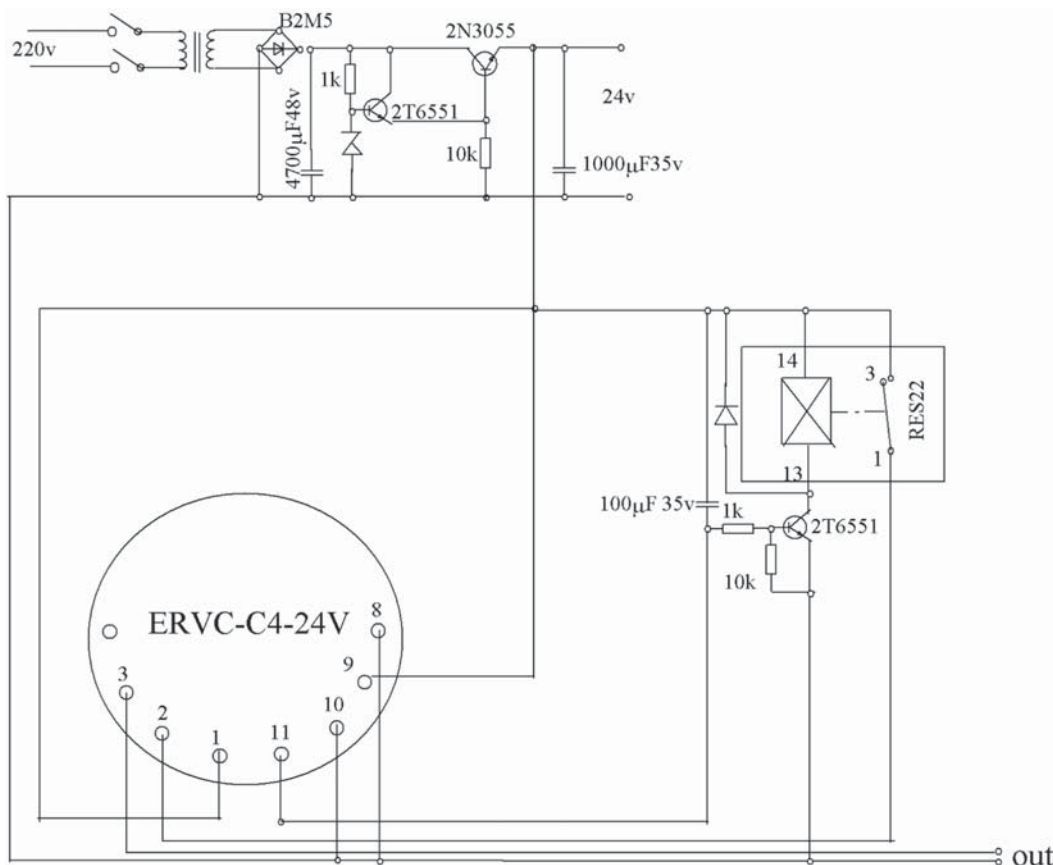


Fig. 3. Power supply and timer blocks

In the opposite case, when $\Delta H < 0$, $\frac{d \ln C}{dT} < 0$, the solubility (C) lowers with temperature (T) and vice versa, as it is shown on Figure 1 with broken line.

For a small temperature interval $\Delta T = T_2 - T_1$ (from the true experimental curve), we can determine the absolute saturation $C_2^0 - C_1^0$ and the relative one –

$$\sigma = \frac{C_2^0 - C_1^0}{C_1^0},$$

where C^0 is the corresponding equilibrium concentration for a given temperature T.

At greater temperature intervals of cooling $\Delta T = T_i - T_f$, where, T_i – initial temperature, T_f – final temperature of the process, it is possible to determine (from the true dependency $C^0(T)$), the volume of the solid mass which emanates from one mol solution by result of cooling within the chosen temperature interval. The volume of the solid mass is determined by the difference $C_{(T_i)}^0 - C_{(T_f)}^0$. Of course, depending on our practical needs, besides mol-parts, we can choose other units to express the composition. Then, the obtained solid mass will be expressed in the corresponding dimensions.

In the cases where the true dependence $\frac{dC^0}{dT} \rightarrow 0$ this method is inapplicable .

2.2. Apparatuses

Apparatus consist: water – coated (jacketed) thermostat chamber, hermetic vessels with starting solution mixture and electronic hardware. The latter decreases temperature in the chamber by custom rate.

2.3. Hardware

The power supply block and timer are shown in Figure 3. The power supply block consists of transformer 220/30V, diode-bridge B2M5, Zener diode (24 V) and emitter follower, consisting of the transistors 2T6551 and 2N3055. The stabilization coefficient is not high, but fair enough for the schemes supplied. Capacitors 4700 µF/48V and 1000 µF/35V are meant to filter out the oscillations of the input power after a rectifier bridge and make connecting smoother.

The timer is basically a delaying digital relay ERVC-C4-24V and auxiliary relay RES22/RF4500-125. When the supply is turned on, supply voltage

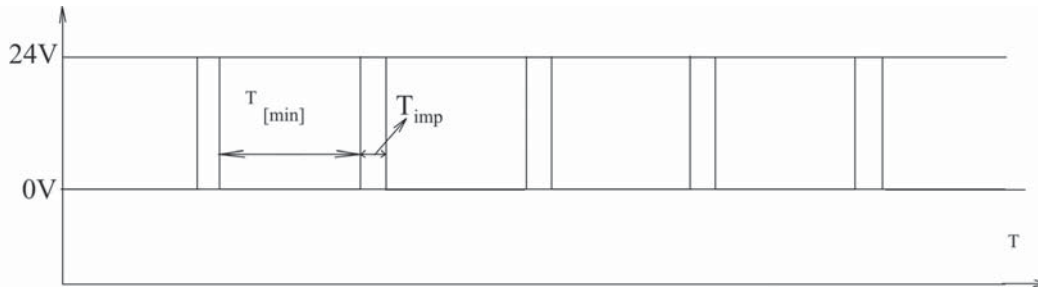


Fig. 4. Output time diagram

reaches ERVC, through the normally closed contact 1–3 of the relay RES22, which is not switched on because the tension on the base of 2T6551 is low. After the delaying relay engages, it switches the contacts from 8–11 to 9–11, at which point tension at the base of 2T6551 becomes high enough (24V) and it is held for a while by the capacitor 100 μ F/35V. Meanwhile RES22 opens the contacts 1–3, the supply for ERVC is cut off and contacts 9–11 switch to 8–11. Then the base of 2T6551 receives low tension, RES22 is left without supply and the contacts 1–3 close the circuit which powers ERVC. With that the cycle is complete. The pulse made by the contacts 1–3 of the relay ERVC is short-living. Its time span is determined by the elements in the basic circuit of 2T6551 – condenser 100 μ F/35V, resistors 10k Ω and 1k Ω , basal current of 2T6551 and the transition processes in the relay system. These processes may not be taken into account, because the R-C elements are chosen in such a way so $T_{imp} > 0,5S$. The generator outputs a pulsating tension, whose time-diagram is shown on Figure 4.

As we mentioned above, T_{imp} is firmly determined by the elements incorporated in the base circuit

of 2T6551. They are chosen in such a way so the system can restart certainly and provide stable work for the pulse magnet and the counter (Fig. 5).

Elements $C = 3600 \mu F/35V$ и $R = 5\Omega$ are included in order to provide reliable work for the pulse magnet (PM). This (PM) moves a stepper dialer which rotates the head of the contact thermometer. They mitigate shock pulsations of the electrical current, which appear whenever the pulse magnet is engaged.

In the case about the relative super-saturation σ , defined by the speed of cooling, there is addition caused by deviation of temperature. It is determined by the expression:

$$\Delta\sigma = \frac{dC^0}{dT} * \Delta T * \frac{1}{C^0}$$

where: $\Delta\sigma$ – deviation of the relative supersaturation, caused by ΔT , dC^0/dT ; ΔT – deviation from the chosen temperature – T_0 .

Apparently, as the dependency $C^0(T)$ goes more sloped and deviation $\Delta T = T - T_0$ becomes greater, so greater will be the fluctuations of super-saturation. Such conditions are unfavorable for crystal-growth

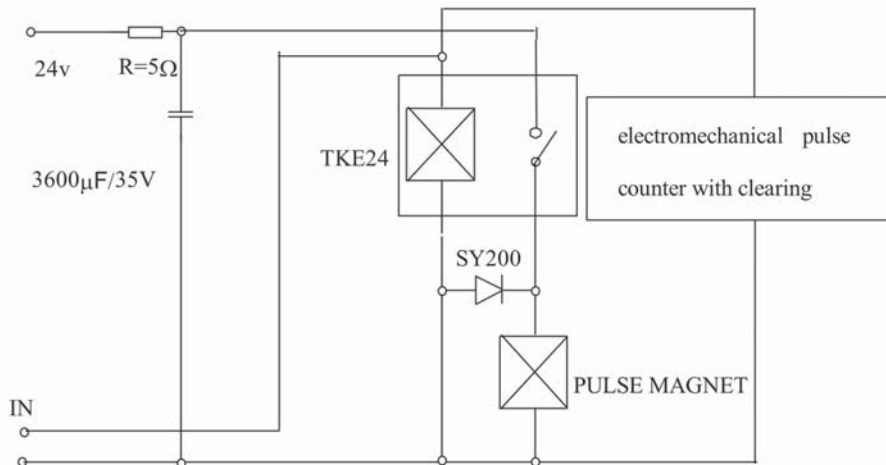


Fig. 5. Scheme of the pulse magnet and counter

from water-based solutions, so measures should be taken to mitigate ΔT . These measures can be as follows:

- Choice of sensor with minimized time for reaction and improvement of the ratio between thermal capacity of thermostatic part and the thermal capacity of the heater.

- Decreasing of the threshold of insensitivity of the sensor (in our case – contact thermometer).

In the case of classic wiring scheme of a contact thermometer when $T > T_{set}$, the electrical current goes through the thermometer and not through the coil of the mercury ampoule. That current $I_{KT} \approx 30$ mA, cannot be lowered in order to keep the circuit safely closed. That circumstance, paired with the induction of the coil and constant temperature, unchanged for long time leads to local soot formation in the capillary tube of the thermometer. That soot formation widens the threshold of insensitivity in the contact zone.

In order to avoid that issue, we have developed a simple and reliable scheme (Fig. 6), which worked without breakdown for more than $2.6 \cdot 10^4$ hours.

The scheme consists of relay type TKE56PODG, TKE21PD, MKU48 or D-KD226B and transistor KT801A. The KD226B keeps the transistor safe from voltage surges during relay shut-down process. The value of the resistor R is determined by the following formula:

$$(24 - U_{eb}) \cdot \beta / I_R$$

where: β – Coefficient of amplification (electrical current) of KT801A in a scheme “common emitter” (≈ 50); I_R – current of engagement of the relay (for

MKU48 ≈ 36 mA); U_{eb} – potential between the emitter and base, which for the most transistors is $U_{eb} \leq 2V$, so:

$$(24 - 2) \cdot 50 / 36 \cdot 10^{-3} \approx 30 \text{ k}\Omega$$

The current through KT can be calculated by the Ohm principle $24V/30 = 0.7$ mA or $7 \cdot 10^{-4}$ A. Voltage over the mercury column is less than 2V. Under these conditions the mercury thermometer is virtually eternal, which is proven by $2.6 \cdot 10^4$ hours of continuous work without any visible change or wear.

2.4. X-ray and SEM apparatuses

For the experiments conducted in Italy, the following apparatuses have been used:

X-ray device and the single-crystal goniometer Siemens P4 four-circle diffractometer with graphite monochromated Mo-K α radiation ($\lambda = 0.71073 \text{ \AA}$) and the $w/2\theta$ scan technique.

The structure was solved by direct methods implemented in the SHELXS-97 program. [G. M. Sheldrick, *SHELXL-97*, Rel. 97-2, Universität Göttingen, 1997]. The refinement was carried out by full-matrix anisotropic least-squares on F^2 for all reflections for non-H atoms by using the SHELXL-97 program. [G. M. Sheldrick, *SHELXL-97*, Rel. 97-2, Universität Göttingen, 1997].

SEM and the EDX probe Philips-501 scanning-electron microscope equipped with an EDAX 9100/60 energy-dispersive analyzer.

3. EXPERIMENTAL RESULTS AND DISCUSSION

3.1. Structure

It is revealed according to data from X-ray analysis conducted in Italy. Unit cell is shown on Figure 7. Analysis has also shown that nickel can isomorphically displace magnesium.

3.2. Density

Data about the density of various samples of magnesium sulfite hexahydrate are shown in Table 1. Density based on calculations about the size of the unit cell has unusually high value than literature data. As is well-known; there are huge objective difficulties of data processing in such cases [5, 6]. Even small inaccuracies can considerably compromise the final results. Future more precise data processing of diffractogramme from X-ray analyses are yet to be done in order to solve these issues.

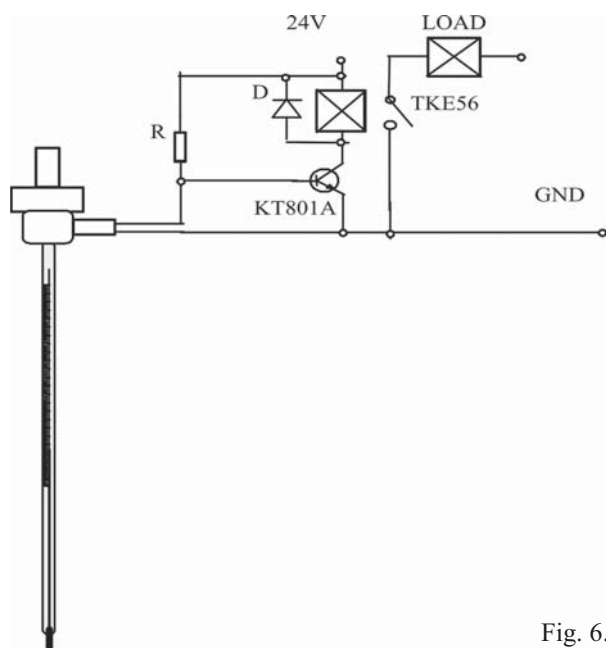
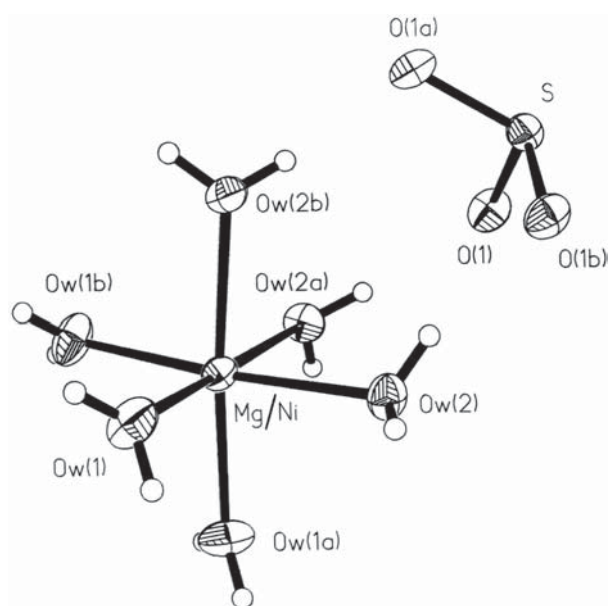


Fig. 6.

Table 1. Density of $\text{MgSO}_3 \cdot 6\text{H}_2\text{O}$

Sample of $\text{MgSO}_3 \cdot 6\text{H}_2\text{O}$	Density [g/cm^3]	Notes, sources
Literature references	1.72	Reference [3]
$\text{MgSO}_3 \cdot 6\text{H}_2\text{O}$ (doped with nickel)	2.151	Calculations based on X-ray analysis made in Italy.
$\text{MgSO}_3 \cdot 6\text{H}_2\text{O}$ (pure)	1.7138	Picnometric measurement made in Sofia University
$\text{MgSO}_3 \cdot 6\text{H}_2\text{O}$ (doped with nickel)	1.7493 ($\pm 0,12\%$)	Picnometric measurement made in Sofia University Crystals doped with nickel show slightly higher density than pure ones.

**Fig. 7.** Unit cell of $\text{MgSO}_3 \cdot 6\text{H}_2\text{O} : \text{Ni}$

We have conducted additional measurement of the density by picnometric method. For the purpose we have used a picnometric vial with volume of 25 cm^3 class “B” made by JENA^{er} GLASS – DDR. The vial is filled with fluid (in our case CCl_4) and then it is weighted on a balance. For the measurement we have used CCl_4 instead of water, because $\text{MgSO}_3 \cdot 6\text{H}_2\text{O}$ has certain solubility in water, which would compromise the final data. Then a crystal sample with known weight is submerged in the fluid and the vial is weighted again. Then the density is calculated with the following formula:

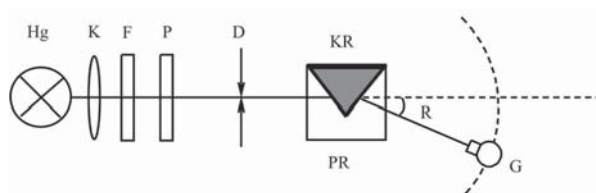
$$\rho = \frac{P}{(P + P_1 - P_2) \cdot \rho_{\text{fluid}}^{-1}}$$

where: P – weight of the crystal sample; P_1 – weight of the vial filled with CCl_4 ; P_2 – weight of the vial filled with CCl_4 and submerged crystal sample; $P + P_1 - P_2$ is the weight of the fluid with volume equal to that of the crystal sample

3.3. Refractive index

It has been measured with refractometer “Pulfrich-PR-2” (made by Carl Zeiss – Jena) and prism ($V_u F3$). Data for the refractive index measurements are shown in Table 2. $\text{MgSO}_3 \cdot 6\text{H}_2\text{O}$ samples doped with nickel show slightly higher refractive indices for a given wavelength than pure samples.

Principal scheme of the refractometer with additional device (polarizer) is shown on Figure 8. The polarizer allows us to measure birefringence of the crystal.

**Fig. 8.** Principal optic scheme of refractometer “Pulfrich-PR-2”, where Hg – mercury lamp; K – collimator; F – filters [λ]; P – polarization filter; D – aperture; KR – $\text{MgSO}_3 \cdot 6\text{H}_2\text{O}$ crystal (blue); PR – prism ($V_u F3$); R – angle of refraction; G – precise goniometer**Table 2.** Refractive indices of $\text{MgSO}_3 \cdot 6\text{H}_2\text{O}$

Wavelength λ [nm]	n_o	n_o	n_e	n_e
	$\text{MgSO}_3 \cdot 6\text{H}_2\text{O}$ (pure)	$\text{MgSO}_3 \cdot 6\text{H}_2\text{O}$ (doped with Ni)	$\text{MgSO}_3 \cdot 6\text{H}_2\text{O}$ (pure)	$\text{MgSO}_3 \cdot 6\text{H}_2\text{O}$ (doped with Ni)
435.8	1.527	1.529	–	–
546.1	1.517	1.519	1.470	1.474

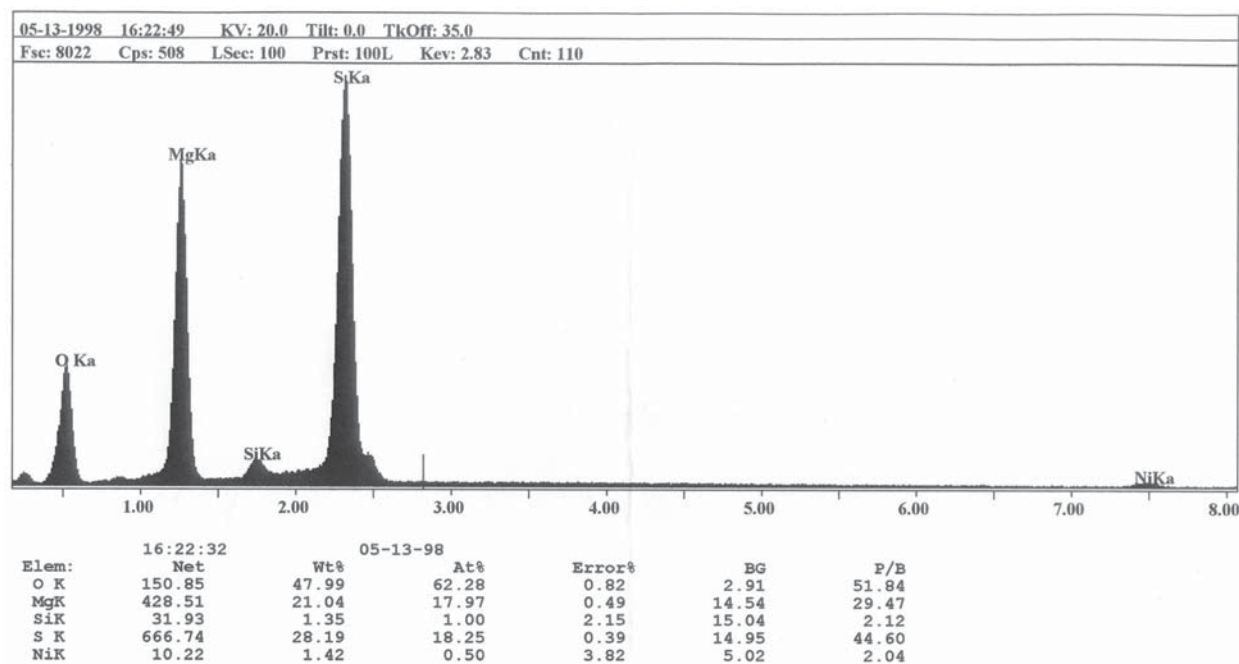


Fig. 9.

These data are in good accordance with the ones obtained previously by us [4] while using indirect method.

Nickel content within the crystals is determined by SEM and X-ray analyses conducted in Italy.

– Mg:Ni ratio results obtained by SEM → Mg: 0,9777; Ni: 0,0223; $\Sigma(\text{Mg}+\text{Ni}) = 1$

– Mg:Ni ratio results obtained by X-ray analysis → Mg: 0,9765; Ni: 0,0235; $\Sigma(\text{Mg}+\text{Ni}) = 1$

Mg:Ni ratio obtained by SEM is shown on Figure 9.

4. CONCLUSION

X-ray analysis has proved that inclusion of Ni is isomorphic on the places of Mg ions and that nickel content is within 2.2% with the latter also being confirmed by SEM analysis. Investigations on density and refractive index have showed that they increase with the presence of nickel.

The difference between density determined by picnometric method – 1.7493 ($\pm 0,12\%$) and calculated from X – ray data – 2.151 is caused by the accepted molecular weight for $\text{NiSO}_3 \cdot 6\text{H}_2\text{O}$, instead proportionally taken between molecular weight of $\text{NiSO}_3 \cdot 6\text{H}_2\text{O}$ ($M=246,865$) and $\text{MgSO}_3 \cdot 6\text{H}_2\text{O}$ ($M=212,47$). Comparison between the values calculated from X–ray data – 2.151 and picnometric data for $\text{NiSO}_3 \cdot 6\text{H}_2\text{O}$ – 2.027 and databases: (ICSD #27807, ICSD #24140, ICSD #26149, ICSD

#48112, PDF24-0739, PDF 01-0473) suggests such conclusion [7–11]. After recalculations according to considerations above we receive value of 1.858 $\text{g}\cdot\text{cm}^3$ – close to real value.

We suppose that $\text{MgSO}_3 \cdot 6\text{H}_2\text{O}$ possesses certain magneto-optic properties, such as refractive index changing under the influence of magnetic field. We hope to confirm that in our future studies. In the future, we expect to obtain similar data about Co-doppant [12–14]. This would help us to clarify these phenomena.

Unfortunately, $\text{MgSO}_3 \cdot 6\text{H}_2\text{O}$ is not stable at temperatures exceeding 55–60 °C, and has certain solubility in water. Sources of heat and humidity from the air may limit its application in optical devices.

Acknowledgements: *The present study is partially supported by Financial support by Bulgarian National Fund project TK-X-1714/07.*

REFERENCES

1. E. Kirkova, Extremely pure compounds, University press “St Kl Ohridski”, Sofia, 1994, 80–102.
2. Ts. Kovachev, Republic of Bulgaria patent N 34515.
3. A. I. Efimov, Properties of non-organic compounds, 1983.
4. Zh. Bunzarov, S. Saltiel, Ts. Kovachev, L. Lyutov, D. Russev, in: Proc. SPIE, 1996, vol. 3052, p. 197.

5. H. W. King, E. A. Payzant, *Canadian Metallurgical Quarterly*, **40**(3), 385 (2001).
6. Q. L. Zhang, W. P. Liu, L. H. Ding, *Chinese Sci. Bull.*, **54**, 3940, doi: 10.1007/s11434-009-0592-6 (2009).
7. H. A. Klasens, W. Perdok, P. Terpstra, *Rec. Trav. Chim. Pays Bas*, **54**, 728 (1935).
8. H. A. Klasens, W. G. Perdok, P. Terpstra, *Z. Krist.*, **94**, 1 (1936).
9. S. Baggio, L. N. Beca, *Acta Cryst. B*, **25**, 1150 (1969).
10. H. Flack, *Acta Cryst. B*, **29**, 656 (1973).
11. L. Andersen, O. Lindqvist, *Acta Cryst. C* **40**, 584 (1984).
12. Zh. Bunzarov, I. Iliev, T. Dimov, P. Petkova, Ts. Kovachev, L. Lyutov, Y. Tzoukrovski, in: Proc. SPIE, 2009, vol. 7501, 75010X.
13. Zh. Bunzarov, I. Iliev, T. Dimov, P. Petkova, *Bulgarian Journal of Chemical Communications*, in press.
14. L. I. Pavlov, G. B. Hadjichristov, S. T. Lazarov, V. K. Kovachev, Z. Bunzarov, I. Buchvarov, I. Nikolov, M. Iliev, in: Proceedings of SPIE, 2007, vol. 6604, p. 66041P1.

МОНОКРИСТАЛИ ОТ МАГНЕЗИЕВ СУЛФИТ ХЕКСАХИДРАТ, ДОТИРАНИ С НИКЕЛ – СТРУКТУРА, ПЛЪТНОСТ И ОПТИЧЕСКИ СВОЙСТВА

Д. Джорджи¹, Г. Л. Лютов², Л. Г. Лютов^{2*}

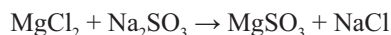
¹ *Университет Сиена, 53100 Сиена, Италия; e-mail: ciads@unisi.it*

² *Софийски Университет „Св. Кл. Охридски“, ул. „Джеймс Баучър“ № 1, София, Bulgaria, e-mail: nhll@chem.uni-sofia.bg*

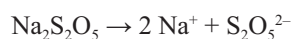
Постъпила на 28 януари, 2011 г.; приета на 22 април, 2011 г.

(Резюме)

MgSO₃·6H₂O е кристално вещество със забележителни оптични свойства, които правят възможно приложението му в съвременните висши технологии. Монокристали от веществото се получават по метод, който представлява комбинация на химическа реакция и политермично израстване от нискотемпературни водни разтвори. Химическата реакция е следната:



За да не настъпи масова кристализация, в системата се прибавят HSO₃⁻ йони, които явно разширяват метастабилната зона и инхибират процеса чрез повишаване на разтворимостта (аналогия – калцит). HSO₃⁻ йони се получават в системата от добавения Na₂S₂O₅ по уравненията.



Растежът на кристалите продължава 20–25 дни, като постепенното понижение на температурата се осъществява от автоматизирано устройство.

Апаратурата позволява получаването на кристали с дължина на ръба на основата на тригоналната пирамида 30–40 mm. Получени са кристали от MgSO₃·6H₂O с включени около 2 до 5% Ni²⁺ йони, като никела е добавен под формата на NiCl₂·6 H₂O.

Проведени са изследвания върху получените за пръв път в световната практика на монокристали от MgSO₃·6H₂O с включени изоморфно Ni²⁺ и Co²⁺ йони. Показано е, че включеният Ni²⁺ повишава коефициента на лъчепречупване и плътността на кристалите, а така също и разликата n_o–n_e. Предполага се, че тези йони биха повлияли и върху магнитооптичните свойства на кристалите.